Glassy Character of DNA Hydration Water

ARTICLE *in* THE JOURNAL OF PHYSICAL CHEMISTRY B · JANUARY 2013

Impact Factor: 3.3 · DOI: 10.1021/jp3105437 · Source: PubMed

6 AUTHORS, INCLUDING:

Andrea Orecchini
Università degli Studi di Perugia
64 PUBLICATIONS **442** CITATIONS
SEE PROFILE

Guido Goracci
Center of Materials Physics
3 PUBLICATIONS **4** CITATIONS
SEE PROFILE

THE JOURNAL OF PHYSICAL CHEMISTRY B

Article

pubs.acs.org/JPCB

Glassy Character of DNA Hydration Water

Alessandro Paciaroni,*[,†,‡] Andrea Orecchini,[†,‡,§] Guido Goracci,[†] Elena Cornicchi,[†] Caterina Petrillo,[†,‡] and Francesco Sacchetti[†,‡]

[†]Dipartimento di Fisica, Università degli Studi di Perugia, Via Pascoli I-06123 Perugia, Italy

[‡]Istituto Officina dei Materiali, Unità di Perugia, c/o Dipartimento di Fisica, Università di Perugia, I-06123 Perugia, Italy

[§]Institut Laue Langevin, 6 rue J. Horowitz F-38042 Grenoble, France

ABSTRACT: The coherent excitations of DNA hydration water at 100 K have been investigated by neutron scattering spectroscopy to extract the excess signal of D_2O-hydrated DNA with respect to dry DNA samples. A structural characterization of the sample, through the analysis of the static structure factor, has suggested that DNA hydration water is largely in an amorphous state up to high hydration degree, with only a small contribution coming from slightly deformed crystalline ice. To describe the inelastic spectra of DNA hydration water, we exploited a phenomenological model already applied in similar disordered systems, such as bulk water (Sacchetti et al. *Phys. Rev. E* **2004**, *69*, 061203; Petrillo et al. *Phys. Rev. E* **2000**, *62*, 3611−3618; Sette et al. *Phys. Rev. Lett.* **1996**, *77*, 83−86) and protein hydration water (Orecchini et al. *J. Am. Chem. Soc.* **2009**, *131*, 4664−4669). Over the low-energy range, the coherent dynamics of DNA hydration water is characterized by a branch at about 7.5 meV, a value slightly larger than that of bulk water. An additional mode in the energy range 20−35 meV is found, with a wavevector dependence seemingly connected with the structural features of amorphous ice. The ensemble of the results supports the glassy nature of DNA hydration water.

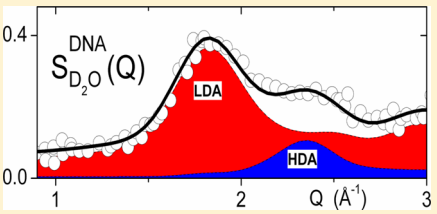

INTRODUCTION

Water plays a key role in modulating the structure and ensuring the stability of nucleic acids. One of the most noticeable hydration-dependent effects is the well-known structural transition between the A- and B-form in DNA.[3] More recently, it has been suggested that changes of the hydration shell may alter the DNA shape in a sequence-dependent manner.[4] Hydration may also affect the recognition process. For instance, highly structured water molecules seem to bridge the ligand to the DNA minor groove without loss of binding affinity.[5] On the other hand, both structural organization and mobility of solvent in the immediate vicinity of biological macromolecules differ from the bulk solvent. In terms of microscopic interactions, the overall behavior is explained by local interactions within the first layer, namely, hydrogen bonding between water molecules and DNA groups and/or among water molecules, and by long-range Coulomb forces originating from (partially) charged groups of the DNA structure, the counterions of DNA, and the water dipoles. Several experimental techniques, including X-ray crystallography[6] and NMR,[7] as well as molecular dynamics simulation studies,[8] have been used to study the properties of water molecules bound to DNA.

The fast dynamics of DNA hydration water is also strongly altered with respect to pure water. Picosecond and nanosecond motions of water molecules at the interface with DNA are characterized by single-particle fluctuations[9,10] that are coupled to the structural fluctuations of the DNA itself. Several experimental investigations[11−14] and MD simulation studies[15,16] have shown that the reorientational dynamics and the diffusive rate of water at the surface of DNA are markedly slowed down. Also, the vibrational features of DNA hydration water are considerably different from the bulk state, as shown by inelastic neutron scattering measurements,[17−19] which were considered an efficient way to derive valuable information on the role of water in the complex interfacial environment. Indeed, by using specific spectral features of the vibrational density of states of hydrated DNA samples, namely, the librational band[17] and the O−H stretching peak,[19] the existence of a large fraction of interfacial water has been clearly shown with many different forms of hydrogen bonding networks.

On the other hand, much less is known about the collective dynamics of water coupled at the DNA interface, despite the fact that phonon-like excitations are sustained by nucleic acid−water systems.[20−23] Very recently, a Brillouin coherent neutron scattering experiment has shown that at room temperature the collective dynamics of DNA hydration water shows vibrational features rather similar to that of bulk water.[24] At small wavevectors ($0.3\ \text{Å}^{-1} \le Q \le 1.5\ \text{Å}^{-1}$), two collective modes were found to be sustained by the aqueous solvent: a first one placed at about 6 meV and a second propagating excitation characterized by a speed of about 3500 m/s. These results globally agree with those previously found for the coherent excitations in bulk water,[1] although in DNA hydration water the speed of propagating modes is definitely higher than that of the pure solvent. Surprisingly, this behavior is also similar to that found for the hydration water of proteins,[2] despite the fact

Received: October 24, 2012
Revised: December 23, 2012
Published: January 8, 2013

that interfacial water in these biomolecules is less strongly bound than in nucleic acids. Another feature common to the hydration water of both DNA and protein is the rapid overdamping of the high-frequency mode, which corresponds to a shorter mean free path than in bulk water for the relevant excitations.[2,24] This phenomenon suggests that hydration water of biomolecules displays a glass-like behavior as far as collective modes are concerned.

On these grounds, to deepen our knowledge on the coherent excitations in DNA hydration water and better characterize its glass-like character, we performed a neutron scattering investigation of dry and hydrated DNA at lower temperature (100 K) and larger wavevectors (1.5 Å^{-1} ≤ Q ≤ 5.5 Å^{-1}). At such a low temperature, we could distinguish the amorphous-ice-like contribution of hydration water from a much less intense crystal-ice-like term. This information allowed us to interpret the coherent inelastic features related to collective dynamics with a phenomenological model we already used in disordered systems,[2,24−26] with a minimum contribution from anharmonic effects. We show that these coherent excitations show a Q-dependent trend that is related to amorphous ice, thus giving further support for the glassy character of an extended shell of DNA hydration water.

MATERIALS AND METHODS

Sample Preparation. DNA from salmon tests was purchased from Sigma-Aldrich (St. Louis, MO). About 0.5 g of DNA was left in 20 g of D_2O (Sigma) for 1 day, in order to properly substitute with deuterium all the exchangeable hydrogen atoms,[27] that is, those belonging to NH, NH_2, and OH groups. Then, the DNA + D_2O mixture was completely dehydrated under a vacuum in the presence of P_2O_5. Such a procedure was repeated three times. Finally, the hydration level h (h = grams D_2O/grams DNA) was achieved by dehydrating the aqueous sample while checking its weight, thus obtaining a wet (1.2 h) and a dry (0.0 h) sample. The hydration level of the wet sample is such that DNA is in the B-form,[28] i.e., in the most common physiological conformation. It is also worth noticing that the hydration level of 1.2 h corresponds to the primary shell around DNA.[29]

Neutron Scattering Experiment. The measurements were performed at 100 K using the time-of-flight spectrometer IN4 of the Institut Laue-Langevin (Grenoble, France). The samples were held in a flat aluminum cell, with an inner thickness of 0.5 cm. The data were collected at two different incident neutron wavelengths, namely, λ = 1.1 and 2.2 Å, corresponding to incident energies of about 67.5 and 16.9 meV and energy resolutions of 3.5 and 0.8 meV (full width at half-maximum), respectively. A good counting statistics was achieved between Q = 2.0 and 5.5 Å^{-1} for λ = 1.1 Å and between Q = 1.25 and 2.5 Å^{-1} for λ = 2.2 Å. The data were corrected applying a standard procedure that takes into account incident flux, sample transmission, cell scattering, environmental background, and different detector efficiencies.

Coherent and Incoherent Neutron Scattering. In a neutron scattering experiment, the observed intensity is analyzed in terms of energy transfer E and momentum transfer $\hbar\mathbf{Q}$, to obtain the dynamic structure factor $S(\mathbf{Q}, E)$. This quantity gives information on the characteristic correlation times and on the spatial geometry of the observed molecular motions, through the dependence on E and $\mathbf{Q}$, respectively.[30] Due to the isotropic nature of our samples, the $\mathbf{Q}$ dependence of the dynamical structure factor is reduced to the sole wavevector modulus Q.

The experimental dynamic structure factor is composed of a coherent and an incoherent contribution, bearing information about single-particle and collective dynamics, respectively. In the case of the present samples, the main contribution from the nucleic acid has a prevalently incoherent nature, because about 30% of DNA is composed of hydrogen atoms: these have a very large incoherent neutron cross section (about 80 barns per atom for thermal neutrons), which overcomes by far both the coherent component of hydrogen and the total cross section of all the other protein atoms (∼5 barns for C, O, N, and S). It is also worth mentioning that the coherent contribution from DNA is partially suppressed by the negative value of the coherent scattering length of hydrogen. On the other hand, the scattering signal produced by D_2O molecules is mostly coherent, thus bearing information about the collective dynamics of the hydration shell.

At a given wavevector $Q \sim 2\pi/d$, where d is the characteristic distance correspondingly probed, the coherent dynamic structure factor is the frequency spectrum of the density fluctuation correlations. Differently from an ideal crystal, where the spectrum of the density fluctuation correlations is related to well-defined $\mathbf{Q}$-dependent phonon (normal) modes, in the present disordered system, the constant-Q spectra are characterized by rather broadened inelastic features. The observed line width is connected to the finite lifetime of the vibrational excitations, which can be due to both structural disorder and interaction with other excitations.

The incoherent contribution coming from the DNA macromolecule appears as a broadening of the elastic peak, the so-called quasielastic scattering, which is characterized by a full width at half-maximum (fwhm) smaller than ∼0.2 meV.[31] This is much narrower than the present experimental energy resolutions (see the Neutron Scattering Experiment section). As a consequence, the quasielastic peak of DNA is fully merged into the resolution-shaped elastic peak and does not contaminate the inelastic spectral region.

On the basis of these observations, we extracted the inelastic coherent contribution of DNA hydration water $S_{D_2O}(Q, E)$ by subtracting the spectrum of the dry sample, $S_{DNA}(Q, E)$, from that of the wet sample, $S_{DNA+D_2O}(Q, E)$, as follows:

$$S_{D_2O}(Q, E) = S_{DNA+D_2O}(Q, E) - \frac{m_{DNA}^{wet}}{m_{DNA}^{dry}} S_{DNA}(Q, E) \quad (1)$$

where m_{DNA}^{dry} and m_{DNA}^{wet} are the masses of DNA in the dry and wet samples, respectively. The inelastic features of the resulting spectra can be mainly ascribed to the coherent density fluctuations of DNA hydration water.

Data Analysis. The inelastic part of the experimental spectra of DNA hydration water was modeled by the sum of damped harmonic oscillator (DHO) functions. As the quasielastic response of the system is known to be narrower than the instrumental resolution, it was taken into account by adding an energy delta-function to the model. The resulting total fit function was finally convoluted with the energy resolution function $R(E)$, that is a Gaussian function of suited fwhm (see the "Neutron Scattering Experiment" subsection). As a whole, the model $S_{mod}(Q, E)$ reads

dx.doi.org/10.1021/jp3105437 | J. Phys. Chem. B 2013, 117, 2026−2031

$$S_{\mathrm{mod}}(Q, E) = \{a(Q)\delta(E) + [n(E) + 1]\cdot \sum_{i=1}^{N} \mathrm{DHO}_i(Q, E)\} \quad (2)$$

where $a(Q)$ is the intensity of the Delta function $\delta(E)$, accounting for both the elastic and quasielastic contributions, and $n(E) = 1/(e^{E/k_BT} - 1)$ is the Bose factor. The number N of DHO functions employed in the fitting procedure depends on the sample and on the energy-transfer range of the analyzed data set.

Each DHO function reads

$$\mathrm{DHO}_i(Q, E) = \frac{a_i(Q)\Gamma_i(Q)E}{(E^2 - \Omega_i^2(Q))^2 + (\Gamma_i(Q)E)^2} \quad (3)$$

where $a_i(Q)$ is a weight factor, $\Omega_i(Q)$ is the oscillation energy, and $\Gamma_i(Q)$ is the damping factor of the ith component. The DHO function is commonly applied to model acoustic collective excitations in the low-Q range in fluids[32] and in previous investigations on similar systems[1,2,24−26] and thus to determine the dispersion curves $\Omega(Q)$ vs Q. Each DHO term can be regarded as a broad, almost continuous distribution of density fluctuations arising from motions of hydration water molecules which experience a large variety of geometrical environments and degrees of freedom. In more detail, the model in eq 2 has already been employed in the investigation of the collective dynamics of complex biological systems, such as hydrated phospholipid bilayers[33−35] and lipid membranes.[36] More recently, it allowed the successful interpretation of neutron scattering data of RNase and DNA hydration water at room temperature.[2,24]

RESULTS

Before discussing the collective dynamics of DNA hydration water, we analyze here the structural properties of the investigated samples as deduced by the present experimental data, which is essential for a better understanding of the dynamical behavior because it provides some more information on the specific arrangement of the interfacial water molecules. Direct information on these properties is obtained from the measured elastic intensity I_{el} of the DNA wet sample, which is shown in Figure 1. Four sharp peaks superimpose over a smooth bump which extends from 30 to 45° and is followed by a weak shoulder between 45 and 55°. A further sharp peak is well visible at about 59°. Such a peak, magnified in the inset of Figure 1, can be tentatively decomposed as the sum of two contributions, namely, at 58.7 and 59.3°. The trend of the elastic intensity can be interpreted as resulting from the superposition of Bragg peaks of crystalline ice with the broad contributions from amorphous ice and the flat incoherent signal from DNA. Information on the crystalline component can be directly obtained by the position of the Bragg peaks. In fact, the presence of a phase of hexagonal ice (Ih) is revealed by the peaks at 2θ = 32.9, 37.4, and 58.7°, which can be assigned to the (100), (101), and (110) reflections.[37] For a closer look, this phase seems to be expanded along the c-direction, as the peak at 34.0° (peak 1) is located at a slightly lower position than expected (34.9°) for the (002) reflection of ordinary Ih ice. Such a structural deformation would correspond to a change of the c lattice parameter from the ordinary value of 7.33 Å to 7.41 ± 0.02 Å. Although the position of the (101) reflection should also be modified by a dilation of the c-axis, the effect on this peak is expected to be much smaller than on the (002) reflection and is indeed not detected with the present experimental angular resolution. On the other hand, peaks 2 and 3 cannot result from the Ih phase, whose basal lattice parameters are supposed to be the same as ordinary hexagonal ice. These peaks likely result from a compressed cubic phase coexisting with the Ih phase, as they are shifted to higher 2θ values than, respectively, the (111) and (220) Bragg peaks of common cubic ice. This compressed phase would be characterized by a lattice parameter a = 6.28 ± 0.02 Å, smaller than the ordinary value of 6.35 Å for Ic.

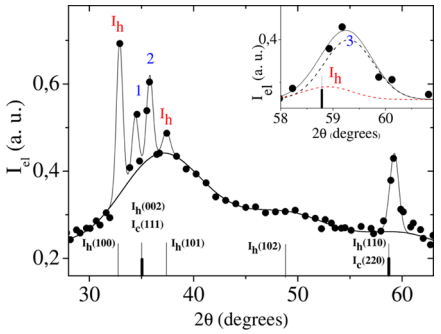

Figure 1. Elastic intensity of DNA hydration water as a function of the scattering angle 2θ. The bottom solid bars indicate the positions of the hexagonal (tiny long lines) and cubic (bold short lines) ice Bragg peaks. The experimental peaks labeled with I_h are those matching the positions of the characteristic Bragg reflection of hexagonal ice. Inset: zoom over the region including the diffraction peaks (110) of I_h and (220) of I_c, which are located at the same 2θ value. The two Gaussian curves (solid red and dashed black lines) are fits to the elastic intensity to individuate the positions of the two peaks labeled with I_h and with 3 (see text).

To investigate the broad amorphous-ice-like contribution found in DNA hydration water, we evaluated the static structure factor $S_{D_2O}^{\mathrm{dis}}(Q)$ of this disordered phase by direct integration of eq 1 over the whole experimental energy range. Besides removing the flat incoherent signal from DNA, accounted for by eq 1, also the elastic component from ice Bragg peaks was taken off. $S_{D_2O}^{\mathrm{dis}}(Q)$ was calculated for Q values lower than 3 Å^{-1} only, as above this value the very strong contribution from the Bragg peaks of the aluminum cell could not be safely subtracted. We interpreted the shape of $S_{D_2O}^{\mathrm{dis}}(Q)$, shown in Figure 2, by a suitable combination of low-density amorphous (LDA), high-density amorphous

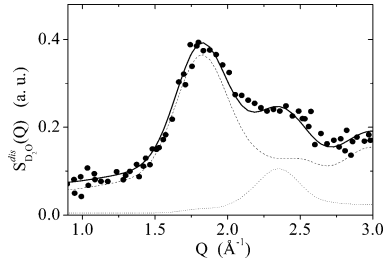

Figure 2. Static structure factor $S_{D_2O}^{\mathrm{dis}}(Q)$ (full circles, measured at the incident wavelength λ = 2.2 Å) estimated as described in the text. Dashed and dotted lines are, respectively, the contributions from low-density amorphous ice and very-high-density (slightly compressed) amorphous ice. The resulting fit to the experimental structure factor is the continuous line.

dx.doi.org/10.1021/jp3105437 | J. Phys. Chem. B 2013, 117, 2026−2031

(HDA), and very-high-density amorphous (vHDA) ice structure factors.[38] It turns out that the best fit to the experimental data results from the combination of an LDA component, slightly shifted to higher Q values by an amount of 0.14 Å^{-1}, plus a smaller vHDA contribution. By integrating the components of this fit, we estimate that low-temperature DNA hydration water is mostly similar to a slightly compressed LDA ice (0.86 h), coexisting with two minority vHDA and crystalline ice phases (0.17 h each). The vibrational dynamics of DNA and its hydration water was investigated by analyzing the inelastic part of the neutron scattering spectra. In Figure 3, we show the

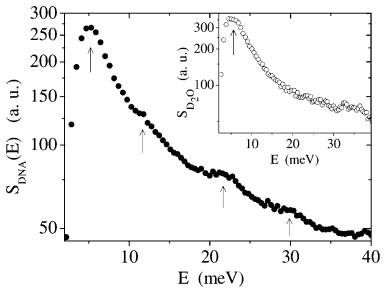

Figure 3. Dynamic structure factor for DNA $S_{DNA}(E)$ integrated over the experimental Q range corresponding to the incident wavelength λ = 2.2 Å. Inset: dynamic structure factor for DNA hydration water $S_{D_2O}(E)$ integrated over the experimental Q range corresponding to the incident wavelength λ = 2.2 Å.

dynamic structure factor of dry DNA, integrated over the whole experimental angular range $S_{DNA}(E)$ after subtraction of the elastic peak to highlight the less intense inelastic features. As the dry DNA sample has a prevailing incoherent signal, $S_{DNA}(E)$ is directly proportional to the vibrational density of states, apart from the $E/n(E)$ factor.[27] Three bumps at about 5, 22, and 30 meV and a broad shoulder in the region 10−15 meV are revealed. In the inset of Figure 3, we also show $S_{D_2O}(E)$. This quantity is much less structured than $S_{DNA}(E)$ and only a defined peak between 4 and 7 meV is visible.

The signal from DNA hydration water is mostly coherent and, as discussed above, comes from a mainly amorphous-like system. It is then more suitably described as a function of Q by using eq 2.[2,24−26,32−35] As shown in Figure 4, three DHO functions are required to properly fit the experimental data at both of the employed energy resolutions. The trend of the excitation energies vs Q, i.e., the dispersion curves, is plotted in Figure 5, together with the excitation energies of DNA hydration water measured in the Q-range 0.2−3.3 Å^{-1} at room temperature.[24] In this figure, we do not show the third DHO contribution, which appears to be centered at high energy around 60 meV and plausibly corresponds to the libration of D_2O molecules.[39]

DISCUSSION

The coexistence of I_c and I_h suggested by Figure 1 has been observed in the past also in samples of hydrated proteins, with gradual conversion of cubic to hexagonal ice as temperature increases.[40] A splitting of some diffraction peaks of hexagonal ice has been observed by X-rays also in pure water and aqueous buffer solutions, where it was ascribed to local stresses created on the ice/ice or ice/container interface during water-to-ice transformation.[41] We can employ the model proposed in ref 38, with an average linear compressibility of 0.01 Å/kbar, to

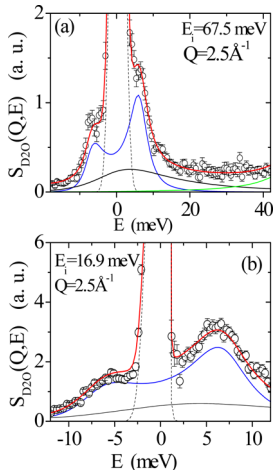

Figure 4. Dynamic structure factor of DNA hydration water at Q = 2.5 Å^{-1}, obtained from the measurements with two different energy resolutions: (a) lower resolution fwhm = 3.5 meV; (b) higher resolution fwhm = 0.8 meV. In both parts, the red line is the global fit to eq 2, the dashed black line is the energy resolution, while the blue, black, and green solid lines are the three DHO functions employed in the fitting procedure.

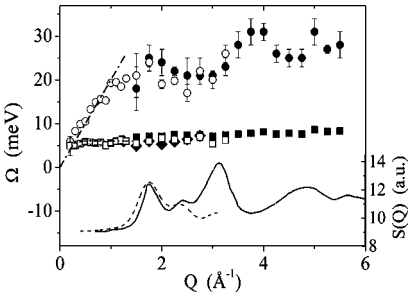

Figure 5. Dispersion curves of DNA hydration water, obtained from the data acquired with two different energy resolutions: fwhm = 3.5 meV (full symbols) and fwhm = 0.8 meV (white rhombs). For comparison, the oscillation energies of the two collective modes of DNA hydration water at 300 K (empty symbols) and of bulk water (dot-dashed lines) are reported. The static structure factor as estimated from a combination of HDA and vHDA ice (see text) is reported (solid line), together with the static structure factor measured in the present experiment (dashed line).

estimate that an effective hydrostatic pressure of about 3.5 kbar is required to explain the observed shift of both I_h and I_c peaks. Both the I_h dilation and the I_c compression might originate from local stresses of ice nanocrystals, due to their interaction with the DNA surface and with the remaining crystalline or amorphous ice phases. The interaction of water molecules with DNA surface groups is also responsible for the existence of the two amorphous states that are traced back in Figure 2. This polyamorphic character is certainly due to the fact that water molecules sense variable electrostatic potentials, because of both the nature of the different solvent-exposed DNA groups and the different geometrical environment of the minor and major grooves. A similar scenario has been recently proposed also for protein hydration water,[42] and more precisely, the formation of HDA or LDA ice has been suggested to be dependent on the hydrophobicity of the specific biomolecular site that actually interacts with the water molecule.[43] The amount 1.03 h of amorphous ice-like hydration water with respect to the full hydration degree of 1.2 h[29] is a direct

dx.doi.org/10.1021/jp3105437 | J. Phys. Chem. B 2013, 117, 2026−2031

estimate of the total amount of water molecules strongly or weakly interacting with the DNA surface.[8,44] This fraction is quite close to the percolation threshold of hydration water on the surface of rigid B-DNA, which is about 0.96 h and has been put in a relationship with the stabilization of the B form and charge transport in DNA.[45] This correspondence suggests that bound hydration water, with a prevalent amorphous ice-like character, is strongly connected to conformational and physical properties of nucleic acids. A complex interfacial water structure, quite different from that of ice Ih, has already been suggested in different investigations[6−8] and inelastic neutron scattering results support this view,[17] indicating also the presence of disordered water molecules which can be found also in DNA crystals. It is also worth noticing that the amorphous character of DNA interfacial water has been suggested in the past on the basis of the analysis of the O−H stretching band as measured by inelastic neutron scattering.[19] In this study, the O−H stretching feature at a hydration degree of 1.2 h was found to result from two Ih and HDA ice components with a relative weight of about 0.5:0.5.[19] The present findings suggest that also the LDA ice contribution to the O−H stretching band should be taken into account, this contribution being centered at an intermediate frequency between Ih and LDA ice.[46]

The incoherent inelastic features shown in Figure 3 fully reproduce the experimental results found with other spectroscopic techniques. The bump at around 5 meV (40 cm^{-1}) and the broad shoulder in the region 10−15 meV have been observed also by Raman scattering[47] and infrared absorption spectroscopy.[48] While the former should be mainly related to interhelical collective modes,[49] the latter would have an intrahelical character, as it originates from the relative displacement of a counterion and the corresponding phosphate group,[49] which can occur either in or out of phase. A predominant intrahelical character would be characteristic of the bumps at 22 and 30 meV, that would respectively originate from the stretching vibration of sugars against the phosphates and from concerted librations among base pairs.[50] The low-frequency bump at 5 meV is the best candidate to be coupled with the low-frequency nondispersive collective mode, observed at about 7.5 meV (see Figure 5). This branch is quite close to an analogous feature found in amorphous ice[51] and slightly above the corresponding excitation of DNA hydration water at room temperature. The latter suggests a moderate stiffening of the system at low temperatures. In bulk water, a similar low-frequency mode has been ascribed to restricted translations perpendicular to the hydrogen bond, O−H···O axis, or O−O−O bending.[52] In DNA hydration water, it can be directly coupled to the interhelical collective motions of DNA mentioned above. The other branch with excitation energy values between 20 and 35 meV seems to be the direct continuation of the acoustic mode measured at room temperature in the Q-range 0.2−3.3 $Å^{-1}$.[24] The nice superposition in this Q-range between room- and low-temperature data indicates that the picosecond collective dynamics is nearly temperature-independent.

An interesting feature of this high-energy branch is its oscillating trend vs Q. To interpret such a trend, we consider that the square of the oscillation frequencies Ω^2 can be well approximated by the normalized second moment of the dynamic structure factor, which is defined by $\langle\omega^2\rangle = 1/S(Q)\int S(Q,\ \omega)\omega^2\,d\omega = Q^2/Mk_BTS(Q)$,[30] where M is an effective mass. It then turns out that Ω is proportional to $QS(Q)^{-1/2}$. In Figure 5, the oscillation frequency dispersion $\Omega(Q)$ is also compared with $S_{D_2O}{}^{dis}(Q)$, as estimated in the present neutron experiment, and with a mixture static structure factor $S_{mix}(Q)$, calculated as a weighted average of X-ray LDA- and vHDA-ice static structure factors,[38] with the same weighing coefficients as in Figure 2. It clearly appears that the Q-dependent modulation of the high-energy branch closely recalls the reciprocal trend of $S_{mix}(Q)$, while the correspondence with $S_{D_2O}{}^{dis}(Q)$ is much less evident, also because of the limited Q-range where it is has been estimated. This result suggests that the collective dynamics of DNA hydration water is dominated by the structural fluctuation of oxygen atoms, that provide the main contribution to $S_{mix}(Q)$. In addition, the inversely proportional relationship between Ω and $S_{mix}(Q)$ further supports the glassy character of DNA hydration water.

The similarity between low-temperature DNA hydration water and amorphous ice can be related to some physical aspects of cryopreservation. It may be speculated that biological tissues embedded in amorphous ice environments are better preserved because such environments resemble the structure of naturally formed DNA hydration water.[53] Actually, the description of the structural and dynamical properties of DNA hydration water, also in the low-temperature regime, is a capital goal in fundamental sciences, ranging from physics[54] to biology[55] and medicine,[56] and it is expected to have a remarkable impact for application in cryobiology and cryopreservation.

■ CONCLUSIONS

The hydration shell of nucleic acids is usually supposed to be structurally and dynamically heterogeneous, as water molecules interact with the atomic groups of phosphate, sugar, and base of DNA, thus sensing a variable polar environment. In addition, also the geometrical constraints felt by water molecules at the DNA surface may change significantly, depending on the structural features of the polynucleotide, e.g., minor and major grooves. In this work, we show that the interaction with DNA is able to markedly alter both the structural and dynamical properties of interfacial water. At low temperature, about 17 water molecules per nucleotide, out of an amount of 20 water molecules corresponding to the full hydration degree (1.2 h), make an amorphous-ice-like structure around the DNA surface. This glassy hydration shell has a polyamorphous character, with structural features that can be interpreted as the combination of a major component reminiscent of LDA ice and a minor component similar to HDA ice. As for the coherent excitations in the THz range, we show that their behavior is different from both bulk water and Ih ice. In particular, the high-energy dispersion branch displays a wavevector dependence that can be put in a close relationship with the structural features of LDA and HDA ice, thus supporting further the glass-like nature of the low-temperature DNA hydration shell.

■ AUTHOR INFORMATION

Corresponding Author

*E-mail: alessandro.paciaroni@fisica.unipg.it.

Notes

The authors declare no competing financial interest.

■ REFERENCES

(1) Sacchetti, F.; Suck, J.-B.; Petrillo, C.; Dorner, B. *Phys. Rev. E* **2004**, *69*, 061203. Petrillo, C.; Sacchetti, F.; Dorner, B.; Suck, J.-B.

Phys. Rev. E **2000**, *62*, 3611−3618. Sette, F.; Ruocco, G.; Krisch, M.; Masciovecchio, C.; Verbeni, R.; Bergmann, U. *Phys. Rev. Lett.* **1996**, *77*, 83−86.
(2) Orecchini, A.; Paciaroni, A.; De Francesco, A.; Petrillo, C.; Sacchetti, F. *J. Am. Chem. Soc.* **2009**, *131*, 4664−4669.
(3) Franklin, R. E.; Gosling, R. G. *Nature* **1953**, *171*, 740−741.
(4) Daisuke, M.; Kaori, N.; Hisae, T.-K.; Tatsuo, O.; Naoki, S. *J. Am. Chem. Soc.* **2009**, *131*, 3522−3531.
(5) Nguyen, B.; Neidle, S.; Wilson, W. D. *Acc. Chem. Res.* **2009**, *42*, 11−21.
(6) Schneider, B.; Cohen, D.; Berman, H. M. *Biopolymers* **1992**, *32*, 725−750.
(7) Halle, B.; Denisov, V. P. *Biopolymers* **1998**, *48*, 210−233.
(8) Feig, M.; Pettitt, B. M. *Biopolymers* **1998**, *48*, 199−209.
(9) Cornicchi, E.; Capponi, S.; Marconi, M.; Onori, G.; Paciaroni, A. *Philos. Mag.* **2007**, *87*, 509−515.
(10) Brauns, E. B.; Madaras, M. L.; Coleman, R. S.; Murphy, C. J.; Berg, M. A. *J. Am. Chem. Soc.* **1999**, *121*, 11644−11649.
(11) Phan, A. T.; Leroy, J. L.; Gueron, M. *J. Mol. Biol.* **1999**, *286*, 505−519.
(12) Pal, S. K.; Zhao, L.; Zewail, A. H. *Proc. Natl. Acad. Sci. U.S.A.* **2003**, *100*, 8113−8118.
(13) Andreatta, D.; Lustres, L. P.; Kovalenko, S. A.; Ernsting, N. P.; Murphy, C. J.; Coleman, R. S.; Berg, M. A. *J. Am. Chem. Soc.* **2005**, *127*, 7270−7271.
(14) Yang, M.; Szyc, Y.; Elsaesser, T. *J. Phys. Chem. B* **2011**, *115*, 13093−13100.
(15) Jana, B.; Pal, S.; Bagchi, B. *J. Phys. Chem. B* **2010**, *114*, 3633−3638.
(16) Makarov, V. A.; Feig, M.; Andrews, B. K.; Pettitt, B. M. *Biophys. J.* **1998**, *75*, 150−158.
(17) Ruffle, S. V.; Michalarias, I.; Li, J.-C.; Ford, R. *J. Am. Chem. Soc.* **2002**, *124*, 565−569.
(18) Michalarias, I.; Beta, I. A.; Li, J.-C.; Ruffle, S. V.; Ford, R. *J. Mol. Liq.* **2002**, *101*, 19−26.
(19) Ilias Michalarias, I.; Gao, X.; Ford, R.; Li, J.-C. *J. Mol. Liq.* **2005**, *117*, 107−116.
(20) Urabe, H.; Hayashi, H.; Tominaga, Y.; Nishimura, Y.; Kubota, K.; Tsuboi, M. *J. Chem. Phys.* **1985**, *82*, 531−535.
(21) Merzel, F.; Fontaine-Vive, F.; Johnson, M. R.; Kearley, G. J. *Phys. Rev. E* **2007**, *76*, 031917.
(22) Krisch, M.; Mermet, A.; Grimm, H.; Forsyth, V. T.; Rupprecht, A. *Phys. Rev. E* **2006**, *73*, 061909.
(23) Liu, Y.; Berti, D.; Faraone, A.; Chen, W. R.; Alatas, A.; Sinn, H.; Alp, E.; Said, A.; Baglioni, P.; Chen, S.-H. *Phys. Chem. Chem. Phys.* **2004**, *6*, 1499−1505.
(24) Cornicchi, E.; Sebastiani, F.; De Francesco, A.; Orecchini, A.; Paciaroni, A.; Petrillo, C.; Sacchetti, F. *J. Chem. Phys.* **2011**, *135* (2), 025101.
(25) Paciaroni, A.; Orecchini, A.; Haertlein, M.; Moulin, M.; Conti Nibali, V.; De Francesco, A.; Petrillo, C.; Sacchetti, F. *J. Phys. Chem. B* **2012**, *116*, 3861−3865.
(26) Orecchini, A.; Paciaroni, A.; Petrillo, C.; Sebastiani, F.; De Francesco, A.; Sacchetti, F. *J. Phys.: Condens. Matter* **2012**, *24*, 064105.
(27) Nakanishi, M.; Tsuboi, M.; Saijo, Y.; Nagamura, T. *FEBS Lett.* **1977**, *81*, 61−64.
(28) Albiser, G.; Lamiri, A.; Premilat, S. *Int. J. Biol. Macromol.* **2001**, *28*, 199−203.
(29) Texter, J. *Prog. Biophys. Mol. Biol.* **1979**, *33*, 83−97.
(30) Lovesey, S. *Theory of Neutron Scattering from Condensed Matter*; Oxford University Press: Oxford, U.K., 1988.
(31) Beta, I. A.; Michalarias, I.; Ford, R. C.; Li, J. C.; Bellissent-Funel, M.-C. *Chem. Phys.* **2003**, *292*, 451−454.
(32) Boon, J.-P.; Yip, S. *Molecular Hydrodynamics*; Dover Publications, Inc.: New York, 1992.
(33) Chen, S. H.; Liao, C. Y.; Huang, H. W.; Weiss, T. M.; Bellisent-Funel, M. C.; Sette, F. *Phys. Rev. Lett.* **2001**, *86*, 740−743.
(34) Weiss, T. M.; Chen, P.-J.; Sinn, H.; Alp, E. E.; Chen, S.-H.; Huang, H.-W. *Biophys. J.* **2003**, *84*, 3767−3776.
(35) Tarek, M.; Tobias, D. J.; Chen, S.-H.; Klein, M. L. *Phys. Rev. Lett.* **2001**, *87*, 238101.
(36) Rheinstädter, M. C.; Ollinger, C.; Fragneto, G.; Demmel, F.; Salditt, T. *Phys. Rev. Lett.* **2004**, *93*, 108107.
(37) Kuhs, W. F.; Lehmann, M. S. *J. Phys. Chem.* **1983**, *87*, 4312−4313.
(38) Tulk, C. A.; Benmore, C. J.; Urquidi, J.; Klug, D. D.; Neuefeind, J.; Tomberli, B.; Egelstaff, P. A. *Science* **2002**, *297*, 1320−1323.
(39) Bellissent-Funel, M.-C.; Chen, S. H.; Zanotti, J.-M. *Phys. Rev. E* **1995**, *51*, 4558−4569.
(40) Sartor, G.; Hallbrucker, A.; Mayer, E. *Biophys. J.* **1995**, *69*, 2679−2694.
(41) Varshney, D. B.; Elliott, J. A.; Gatlin, L. A.; Kumar, S.; Suryanarayanan, R.; Shalaev, E. Y. *J. Phys. Chem. B* **2009**, *113*, 6177−6182.
(42) Paciaroni, A.; Orecchini, A.; Cornicchi, E.; Marconi, M.; Petrillo, C.; Haertlein, M.; Moulin, M.; Schober, H.; Tarek, M.; Sacchetti, F. *Phys. Rev. Lett.* **2008**, *101*, 148104.
(43) Russo, D.; Teixeira, J.; Kneller, L.; Copley, J. R. D.; Ollivier, J.; Perticaroli, S.; Pellegrini, E.; Gonzalez, M. A. *J. Am. Chem. Soc.* **2011**, *133*, 4882−4888.
(44) Umehara, T.; Kuwabara, S.; Mashimo, S. *Biopolymers* **1990**, *30*, 649−656.
(45) Brovchenko, I.; Krukau, A.; Oleinikova, A. *Phys. Rev. Lett.* **2006**, *97*, 137801.
(46) Kolesnikov, A. I.; Li, J.-C.; Parker, S. F.; Eccleston, R. S.; Loong, C.-K. *Phys. Rev. B* **1999**, *59*, 3569−3578.
(47) Urabe, H.; Sugawara, Y.; Ataka, M.; Rupprecht, A. *Biophys. J.* **1998**, *74*, 1533−1540. Weidlich, T.; Lindsay, S. M.; Rui, Q. *J. Biomol. Struct. Dyn.* **1990**, *8*, 139−171.
(48) Wittlin, A.; Genzel, L.; Kremer, F.; Hiseler, S.; Poglitsch, A. *Phys. Rev. A* **1986**, *34*, 493−500.
(49) Chern, L.; Prohofsky, E. W. *Phys. Rev. E* **1992**, *74*, 4483−4495.
(50) Powell, J. W.; Edwards, G. S.; Genzel, L.; Kremer, F.; Wittlin, A. *Phys. Rev. A* **1987**, *35*, 3929−3939.
(51) Schober, H.; Koza, M. M.; Masciovecchio, C.; Sette, F.; Fujara, F. *Phys. Rev. Lett.* **2000**, *85*, 4100−4103.
(52) Walrafen, G. E.; Chu, Y. C. *J. Phys. Chem. B* **1995**, *99*, 11225−11229.
(53) Dubochet, J.; Adrian, M.; Chang, J.-J.; Homo, J.-C.; Lepault, J.; McDowall, A. W.; Schultz, P. *Q. Rev. Biophys.* **1988**, *21*, 129−228.
(54) Kumar, P.; Yan, Z.; Xu, L.; Mazza, M. G.; Buldyrev, S. V.; Chen, S.-H.; Sastry, S.; Stanley, H. E. *Phys. Rev. Lett.* **2006**, *97*, 177802. Chen, S.-H.; Liu, L.; Chu, X.; Zhang, Y.; Fratini, E.; Baglioni, P.; Faraone, A.; Mamontov, E. *J. Chem. Phys.* **2006**, *125*, 171103. Sokolov, A. P.; Grimm, H.; Kahn, R. *J. Chem. Phys.* **1999**, *110*, 7053−7057.
(55) Mazur, P. *Science* **1970**, *168*, 939. Zachariassen, K. E.; Kristiansen, E. *Cryobiology* **2000**, *41*, 257−279.
(56) Mühlbacher, F.; Langer, F.; Mittermayer, C. *Transplant. Proc.* **1999**, *31*, 2069−2070.